

Weighted Intersection over Union (wIoU): A New Evaluation Metric for Image Segmentation

Yeong-Jun Cho

Department of Artificial Intelligence Convergence, Chonnam National University

yj.cho@chonnam.ac.kr

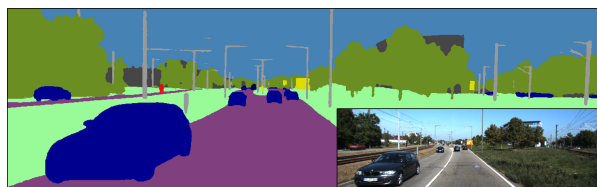
Abstract

In this paper, we propose a novel evaluation metric for performance evaluation of semantic segmentation. In recent years, many studies have tried to train pixel-level classifiers on large-scale image datasets to perform accurate semantic segmentation. The goal of semantic segmentation is to assign a class label of each pixel in the scene. It has various potential applications in computer vision fields e.g., object detection, classification, scene understanding and Etc. To validate the proposed wIoU evaluation metric, we tested state-of-the-art methods on public benchmark datasets (e.g., KITTI, Cityscapes) based on the proposed wIoU metric and compared with other conventional evaluation metrics.

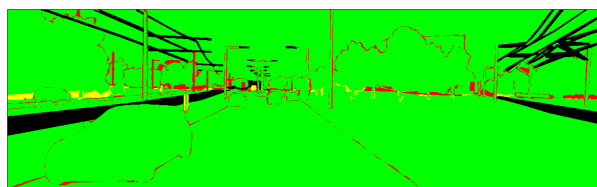
1. Introduction

In recent years, many studies have tried to train pixel-level classifiers on large-scale image datasets to perform accurate semantic image segmentation [27, 31]. The goal of the image segmentation is to assign a class label of each pixel in the scene. It is one of the most basic problems in computer vision fields and has various potential applications e.g., autonomous driving systems [8], scene understanding [21] and medical image diagnostics [15, 17]. Recently, significant advances in deep learning techniques are driving high performance of semantic segmentation in various benchmark datasets [6, 9, 13]. Figure 1 shows a result of the semantic segmentation [31] and its error map in KITTI dataset [13].

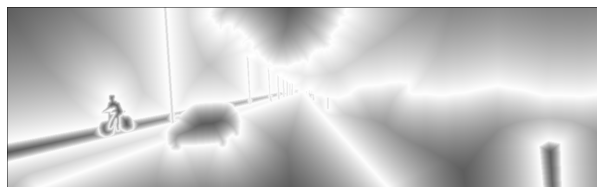
Although the method performs the best compared to other state-of-the-art methods, it still occurs classification errors. Most of errors (i.e., false negatives and positives) occur around object boundaries due to high classification ambiguities around the boundaries as shown in Fig. 1 (b). That is because at least two classes are adjacent around the objects' boundaries making class prediction more difficult and ambiguous. Even though the proportion of boundaries in the scene is very small, it has a significant impact on qual-



(a) Segmentation result [31] with an original image



(b) Error map. Color of each pixel denotes: (green) True positive, (red) False negative, (yellow) False positive, (black) No label.



(c) Proposed weight map for the segmentation evaluation

Figure 1. Challenges in semantic segmentation. It is difficult to predict pixel labels around object boundaries.

itative results. In contrast, the internal areas of objects have relatively low classification ambiguities and occupy most of the scene area.

In recent years, many studies have focused on the importance of the boundary and tried to enhance the classification accuracy based on the boundary information [3, 22, 27]. They added additional network branches in baseline networks and optimized boundary loss terms to exploit the boundary cue. To evaluate semantic segmentation results, most methods [27, 31] rank their methods by measuring intersection-over-union (*IoU*) score described in Sec. 3.2. Unfortunately, *IoU* evaluate all pixels equally. Performance

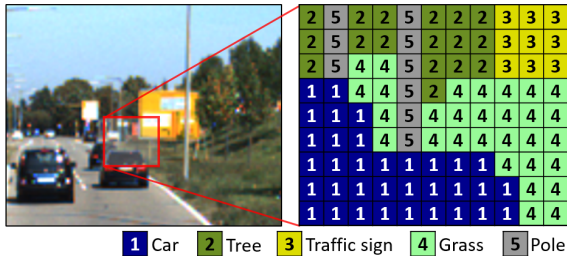


Figure 2. Example of an image and its predicted classes

scores improve very subtly according to the evaluation policy. In order to directly evaluate the boundary estimation results, several evaluation metrics such as BF score [7] and Boundary Jaccard (BJ) [12] were proposed. However.

In this work, we propose a novel evaluation measure for semantic segmentation so-called weighted Intersection over Union ($wIoU$). It first generate weighting map as shown in Fig. 1 (c) based on the proposed weighted map generation.

The contributions of our work are as follows:

- Enable to measure all pixels in an images.
- Scale invariant
- Can evaluate both contour and region
- Does not depend on many hyper-parameters

2. Problem definition

An image segmentation (also called semantic image segmentation) is a problem to find several sub-regions or partitions of the given image in computer vision and digital image processing fields. The sub-regions consist of sets of objects' pixels. The goal of the image segmentation is to predict classes \mathbf{C} of pixels in the given image \mathbf{I} . An image can be represented by a set of pixels as follows,

$$\mathbf{I} = \{i_p | p = (p_x, p_y), 1 \leq p_x \leq W, 1 \leq p_y \leq H\}, \quad (1)$$

where i_p denotes a value of the pixel p . W and H are the width and height of the image, respectively.

In general, an image consists of 3-channel (e.g., R,G,B), but we do not consider the channel index for convenience.

Using given image pixels i_p , the probability distribution of class for each pixel is predicted as $p(c|i_p)$. To predict the probability distribution, we can employ various semantic segmentation approaches [27, 31]. Next, we select the class label of each pixel based on the distributions as follows,

$$c_p^* = \underset{c \in \mathbf{C}}{\operatorname{argmax}} p(c|i_p), \quad (2)$$

| | | Predicted class | |
|--------------|----------|-----------------|----------|
| | | Positive | Negative |
| Actual class | Positive | TP | FN |
| | Negative | FP | TN |

Table 1. Confusion matrix for classification. Blue color indicates correct estimation and red color indicates failure estimation.

where \mathbf{C} is a set of class (e.g., car, tree, road and Etc). Finally, we build a predicted class map of the given image as

$$\mathbf{C} = \{c_p^* | p = (p_x, p_y), 1 \leq p_x \leq W, 1 \leq p_y \leq H\}. \quad (3)$$

Then, $\mathbf{C}(p)$ denotes the class label c at a point $p = (p_x, p_y)$. Figure 2 shows an example of semantic segmentation result with predicted classes. As a result of semantic segmentation, each pixel corresponds to a distinct class label.

3. Related works

3.1. Semantic Image Segmentation Methods

Semantic Image segmentation is one of the most important problem in the computer vision research field. With the recent development of deep learning, many attempts to adopt deep learning into semantic segmentation applications have been presented. R.Girshick *et al.* [14] proposed region proposal convolutional neural networks called R-CNN for object detection and semantic image segmentation. In addition, J. Long *et al.* [20] also proposed a semantic segmentation method via fully convolutional networks (FCN) which is an end-to-end framework performing pixelwise prediction. Thanks to deep neural networks' large model capacity, they improved the prediction performance significantly compared to many popular traditional methods [4, 11, 18, 25, 26] reviewed in [28].

Recently, many methods [3, 5, 19, 22, 27, 29] have focused on the importance of boundary information in the scene to perform accurate semantic segmentation. They added additional network branches and performed boundary loss optimization to capture the boundary information. Then the estimated boundary cues in the scene are effectively employed for semantic segmentation. Many authors insisted that the boundary cue alleviates the boundary blur problem and leads the edge-preserving results. Various benchmark datasets such as PASCAL VOC [9], Cityscapes [6], ADE20K [30], ISPRS2D [1] and KITTI [2, 13] are commonly used to train and evaluate the methods.

3.2. Evaluation Metrics

• **Basic notations for classification results.** To evaluate the results of classification, there are four basic notations according to the actual class and predicted class: (1) True Positive (TP); (2) True Negative (TN); (3) False Positive (FP);

(4) False Negative (FN). Each notation is summarized in Table. 1. TP and TN are correct estimations. FP and FN are false alarms called Type I error and Type II error, respectively.

• **Region-based evaluation.** Based on the types of the classification results, many studies such as machine learning and pattern recognition have evaluated their methods. For example, the evaluation metrics such as Precision and Recall are very widely used: $Precision = \frac{TP}{TP+FP}$, $Recall = \frac{TP}{TP+FN}$, Furthermore, F_1 score which is the weighted average of $Precision$ and $Recall$ has been used as an evaluation metric:

$$F_1 = \frac{2TP}{2TP + FN + FP}, \quad (4)$$

It reflects two evaluation results ($Precision$ and $Recall$) evenly. Another common metric for evaluating classification is a Jaccard index (JI):

$$JI = \frac{TP}{TP + FN + FP}, \quad (5)$$

For semantic image segmentation problem defined in Sec. 2, Intersection over Union (IoU) is equivalent to JI :

$$IoU = JI = \frac{|C \cap C_{gt}|}{|C \cup C_{gt}|} \quad (6)$$

where C denotes a predicted class map and C_{gt} denotes a ground-truth class label map. Most of the previous studies related to semantic segmentation [27, 31] have adopted IoU measure. It compares a similarity between two regions (C and C_{gt}) to evaluate all predicted pixels of the image.

• **Boundary-based evaluation.** Meanwhile, many studies [7, 24] pointed out that the prediction performance on the boundaries of objects has a significant impact on the perceived segmentation quality. In fact, object boundary has higher prediction difficulty than an internal area of the object – At least two classes are adjacent around the objects’ boundaries, which makes class prediction more difficult and ambiguous. However, IoU equally evaluates all pixels in the image making it hard to evaluate performances around object boundaries.

Some studies [23, 24] evaluated the edge prediction results by measuring edge-based F_1 score only around the objects’ edges via bipartite matching. To make the evaluation metric is robust to small error, they set the distance tolerance (θ) for performing bipartite matching between predicted edge points and ground-truth edge points. In addition, BF score [7] and Boundary Jaccard (BJ) [12] also proposed to capture the edge prediction results.

The evaluation metrics can measure the boundary prediction performance; however they still require certain distance tolerance values (θ), which determines the boundary

| | IoU | [7] | [12] | $wIoU$ |
|-----------------|-------|-----|------|--------|
| Scale invariant | ✓ | - | - | ✓ |
| issue 2 | - | - | - | ✓ |
| issue 3 | - | - | - | ✓ |

Table 2. Comparison of methods (temporary).

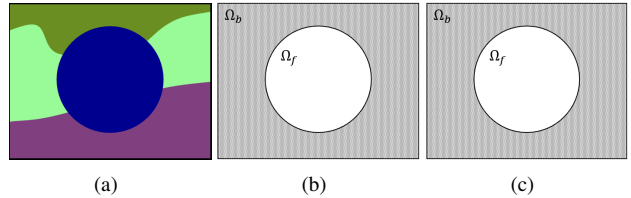


Figure 3. (a) Example of a ground-truth class map C_{gt} . (b) Corresponding foreground (Ω_c^f) and background (Ω_c^b) regions where $c = 1$. Solid blue line is the boundary of the object.

region in the scene. Selecting a distance tolerance (θ) occurs an inflexibility in evaluation measures. Furthermore, region-based evaluation metrics and boundary-based evaluated metrics are separated to make it difficult to compare the image segmentation performances at a glance. In this study, we propose a single evaluation metric that can measure both evaluation factors (i.e., region- and boundary-based) in Sec. 4.

4. Proposed Evaluation Metric

4.1. Motivation and main ideas

(Will be modified) It is more difficult to infer the label of the boundary of each object. This is because the inference probability of each label is mixed at the boundary. Unfortunately, the details of an object are usually at the boundary. Even if most of the object region is predicted, if it fails to predict the boundary of the object, it looks qualitatively bad. In addition, missing object details can lead to poor results in applications of semantic segmentation. Techniques for measuring the performance of existing semantic segmentation. Therefore, in this study, we evaluate the gain of the pixels close to the boundary of the object.

We exploit a distance transform map as a weighted field.

4.2. Weighted map generation

The problem of a distance transform is to compute the distance of each point from the boundary of foreground region [10]. First, it assigns fore- and back-ground regions according to the class label c as

$$\Omega_c^f = \{p | C_{gt}(p) = c\}, \Omega_c^b = \{q | C_{gt}(q) \neq c\}. \quad (7)$$

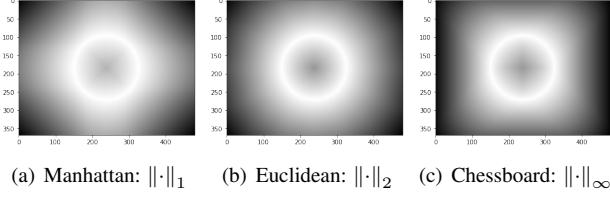


Figure 4. Distance maps according to ρ -norm distance metrics. Bright pixel indicates a large distance. First row (a-c) and second row (d-f).

Each region consists of a set of points. Figure 3 shows predicted map (\mathbf{C}) (Fig. 3 (a)) and its corresponding foreground and background regions (Ω_c^f, Ω_c^b) where $c = 1$ and $c = 4$ (e.g., Fig. 3 (b) and (c)). The boundary of each region is the boundary of the object.

Next, it generates a distance map \mathbf{D}_c that consists of a distance value of each point p by computing the smallest distance from the background region Ω_c^b . It is represented by

$$\mathbf{D}_c(p) := \min \{d(p, q) \mid p \in \Omega_c^f, q \in \Omega_c^b\}, \quad (8)$$

where $d(p, q)$ is the pixel distance between two points p and q . To compute the distance, we can adopt the ρ -norm (also called l_ρ norm) defined by

$$\begin{aligned} d(p, q) &:= \|p - q\|_\rho \\ &= (|p_x - q_x|^\rho + |p_y - q_y|^\rho)^{\frac{1}{\rho}}. \end{aligned} \quad (9)$$

where $\rho \geq 1$. As shown in Fig. 4, ρ -norm generates various distance metrics such as Manhattan ($\rho = 1$), Euclidean ($\rho = 2$), and Chessboard ($\rho = \infty$) distances according to its value ρ . In this work, we set ρ as 2 to follow Euclidean distance for generating the weight map \mathbf{D}_c . As it mentioned in Sec 4.1, we aim to generate a weight map according to the distance from the object boundary. Calculating Euclidean distance can efficiently approximate to compute the normal distances from the boundaries. As a result, distance maps for all categories \mathcal{C} can be simply calculated.

However, distance map of each object has different distance range due to the difference in size between the objects. It causes unfair performance evaluation in many cases [?]. To handle the challenge, we designed the regularized distance as

$$\bar{\mathbf{D}}_c(p) = \frac{\mathbf{D}_c(p)}{\max(\mathbf{D}_c(p))}. \quad (10)$$

Then it lies on $[0, 1]$ for all pixel points p and classes c . Considering all the class in the class map \mathbf{C} , the distance maps $\bar{\mathbf{D}}_c$ can be combined into one distance map as follows

$$\bar{\mathbf{D}}(p) = \{\bar{\mathbf{D}}_c(p) \mid 1 \leq c \leq \mathcal{C}\}, \quad (11)$$

Algorithm 1: Algorithms will be written.

```

Result: Write here the result
initialization;
while While condition do
  instructions;
  if condition then
    instructions1;
    instructions2;
  else
    instructions3;
  end
end

```

Finally, a weight map is calculated by

$$\mathbf{W}(p) = e^{-\alpha \bar{\mathbf{D}}(p)}, \quad (12)$$

where $\alpha > 0$ is an boundary importance factor. As shown in Fig. 5, the value of α determines the importance of boundaries in the scene. When the boundary importance is small ($\alpha = 0.01$), the weight map is uniformly distributed (Fig. 5 (a)). It means that all areas have about the same weights. On the other hand, when the boundary importance is comparatively large ($\alpha = 100$), it emphasizes only the boundaries in the scene (Fig. 5 (e)). In this way, we can set the weight map very simply by manipulating only one parameter α .

4.3. Weighted intersection over union

Based on the calculated weight map in Sec. 4.2, we propose a new evaluation metric: Weighted Intersection over Union (wIoU) as follows

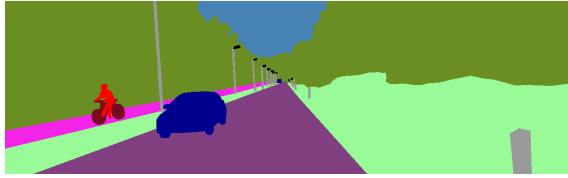
$$wIoU = \frac{|\mathbf{C} \cap (\mathbf{C}_{gt} \circ \mathbf{W})|}{|\mathbf{C} \cup (\mathbf{C}_{gt} \circ \mathbf{W})|} \quad (13)$$

where \circ is an element-wise product called Hadamard product [16]. In this step, we omit p for convenience and all terms in the Eq. 13 have the same dimension (i.e., size of an input image). Comparing the proposed wIoU with conventional IoU (Eq. 6), it emphasizes the importance of each pixel based on the weight map \mathbf{W} . The overall process to evaluate semantic segmentation using $wIoU$ is described in Algorithm 1.

5. Experimental Results

6. Conclusions

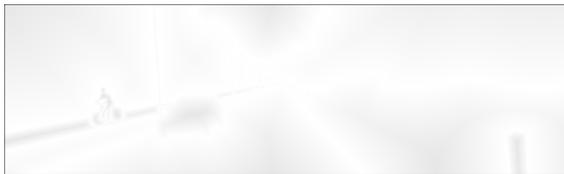
In this paper, we propose a novel evaluation metric for performance evaluation of semantic segmentation. In recent years, many studies have tried to train pixel-level classifiers on large-scale image datasets to perform accurate semantic segmentation. The goal of semantic segmentation is to



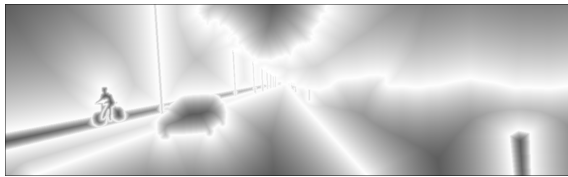
(a) Ground truth C_{gt}



(b) Weight map \mathbf{W} , $\alpha = 0.01$



(c) Weight map \mathbf{W} , $\alpha = 0.1$



(d) Weight map \mathbf{W} , $\alpha = 1$



(e) Weight map \mathbf{W} , $\alpha = 10$



(f) Weight map \mathbf{W} , $\alpha = 100$

Figure 5. Ground truth and its weight maps according to α values. When the value of α is small, weight of each pixel is uniformly distributed. The weights of boundary areas are proportional to the value of α .

assign a class label of each pixel in the scene.+ It has various potential applications in computer vision fields e.g., ob-

ject detection, classification, scene understanding and Etc. To validate the proposed wIoU evaluation metric, we tested state-of-the-art methods on public benchmark datasets (e.g., KITTI, $\circ\circ\circ$) based on the proposed wIoU metric and compared with other conventional evaluation metrics.

References

- [1] Isprs 2d semantic labeling contest. In *Available online: <http://www2.isprs.org/commissions/comm3/wg4/2d-sem-label-vaihingen.html>*, 2018. 2
- [2] H. Alhaja, S. Mustikovela, L. Mescheder, A. Geiger, and C. Rother. Augmented reality meets computer vision: Efficient data generation for urban driving scenes. *International Journal of Computer Vision*, 2018. 2
- [3] G. Bertasius, J. Shi, and L. Torresani. Semantic segmentation with boundary neural fields. In *IEEE Conference on Computer Vision and Pattern Recognition*, June 2016. 1, 2
- [4] J. Carreira and C. Sminchisescu. Constrained parametric min-cuts for automatic object segmentation. In *IEEE Conference on Computer Vision and Pattern Recognition*, pages 3241–3248, 2010. 2
- [5] D. Cheng, G. Meng, S. Xiang, and C. Pan. Fusionnet: Edge aware deep convolutional networks for semantic segmentation of remote sensing harbor images. *IEEE Journal of Selected Topics in Applied Earth Observations and Remote Sensing*, 10(12):5769–5783, 2017. 2
- [6] M. Cordts, M. Omran, S. Ramos, T. Rehfeld, M. Enzweiler, R. Benenson, U. Franke, S. Roth, and B. Schiele. The cityscapes dataset for semantic urban scene understanding. In *IEEE conference on Computer Vision and Pattern Recognition*, pages 3213–3223, 2016. 1, 2
- [7] G. Csarka, D. Larlus, F. Perronnin, and F. Meylan. What is a good evaluation measure for semantic segmentation?. In *British Machine Vision Conference*, 2013. 2, 3
- [8] L. Deng, M. Yang, H. Li, T. Li, B. Hu, and C. Wang. Restricted deformable convolution-based road scene semantic segmentation using surround view cameras. *IEEE Transactions on Intelligent Transportation Systems*, 2019. 1
- [9] M. Everingham, L. Van Gool, C. K. Williams, J. Winn, and A. Zisserman. The pascal visual object classes (voc) challenge. *International Journal of Computer Vision*, 88(2):303–338, 2010. 1, 2
- [10] R. Fabbri, L. D. F. Costa, J. C. Torelli, and O. M. Bruno. 2d euclidean distance transform algorithms: A comparative survey. *ACM Computing Surveys (CSUR)*, 40(1):1–44, 2008. 3
- [11] P. F. Felzenszwalb and D. P. Huttenlocher. Efficient graph-based image segmentation. *International Journal of Computer Vision*, 59(2):167–181, 2004. 2
- [12] E. Fernandez-Moral, R. Martins, D. Wolf, and P. Rives. A new metric for evaluating semantic segmentation: leveraging global and contour accuracy. In *IEEE Intelligent Vehicles Symposium*, 2018. 2, 3
- [13] A. Geiger, P. Lenz, and R. Urtasun. Are we ready for autonomous driving? the kitti vision benchmark suite. In *IEEE Conference on Computer Vision and Pattern Recognition*, 2012. 1, 2

- [14] R. Girshick, J. Donahue, T. Darrell, and J. Malik. Rich feature hierarchies for accurate object detection and semantic segmentation. In *IEEE Conference on Computer Vision and Pattern Recognition*, pages 580–587, 2014. 2
- [15] M. H. Hesamian, W. Jia, X. He, and P. Kennedy. Deep learning techniques for medical image segmentation: Achievements and challenges. *Journal of digital imaging*, 32(4):582–596, 2019. 1
- [16] R. A. Horn. The hadamard product. In *Proc. Symp. Appl. Math*, volume 40, pages 87–169, 1990. 4
- [17] B. Kayalibay, G. Jensen, and P. van der Smagt. Cnn-based segmentation of medical imaging data. *arXiv preprint arXiv:1701.03056*, 2017. 1
- [18] L. Ladický, C. Russell, P. Kohli, and P. H. Torr. Associative hierarchical crfs for object class image segmentation. In *IEEE International Conference on Computer Vision*, pages 739–746, 2009. 2
- [19] S. Liu, W. Ding, C. Liu, Y. Liu, Y. Wang, and H. Li. Ern: Edge loss reinforced semantic segmentation network for remote sensing images. *Remote Sensing*, 10(9):1339, 2018. 2
- [20] J. Long, E. Shelhamer, and T. Darrell. Fully convolutional networks for semantic segmentation. In *IEEE Conference on Computer Vision and Pattern Recognition*, pages 3431–3440, 2015. 2
- [21] M. Malinowski and M. Fritz. A multi-world approach to question answering about real-world scenes based on uncertain input. In *Advances in neural information processing systems*, pages 1682–1690, 2014. 1
- [22] D. Marmanis, K. Schindler, J. D. Wegner, S. Galliani, M. Datcu, and U. Stilla. Classification with an edge: Improving semantic image segmentation with boundary detection. *ISPRS Journal of Photogrammetry and Remote Sensing*, 135:158–172, 2018. 1, 2
- [23] D. R. Martin, C. C. Fowlkes, and J. Malik. Learning to detect natural image boundaries using local brightness, color, and texture cues. *IEEE Transactions on Pattern Analysis & Machine Intelligence (TPAMI)*, (5):530–549, 2004. 3
- [24] F. Perazzi, J. Pont-Tuset, B. McWilliams, L. Van Gool, M. Gross, and A. Sorkine-Hornung. A benchmark dataset and evaluation methodology for video object segmentation. In *IEEE Conference on Computer Vision and Pattern Recognition*, 2016. 3
- [25] J. B. Roerdink and A. Meijster. The watershed transform: Definitions, algorithms and parallelization strategies. *Fundamenta Informaticae*, 41(1, 2):187–228, 2000. 2
- [26] J. Shotton, J. Winn, C. Rother, and A. Criminisi. Textonboost: Joint appearance, shape and context modeling for multi-class object recognition and segmentation. In *European Conference on Computer Vision*, pages 1–15. Springer, 2006. 2
- [27] T. Takikawa, D. Acuna, V. Jampani, and S. Fidler. Gated-scnn: Gated shape cnns for semantic segmentation. In *IEEE Conference on Computer Vision and Pattern Recognition*, pages 5229–5238, 2019. 1, 2, 3
- [28] M. Thoma. A survey of semantic segmentation. *arXiv preprint arXiv:1602.06541*, 2016. 2
- [29] Y. Yuan, J. Xie, X. Chen, and J. Wang. Segfix: Model-agnostic boundary refinement for segmentation. In *European Conference on Computer Vision*, pages 489–506. Springer, 2020. 2
- [30] B. Zhou, H. Zhao, X. Puig, S. Fidler, A. Barriuso, and A. Torralba. Scene parsing through ade20k dataset. In *IEEE conference on Computer Vision and Pattern Recognition*, pages 633–641, 2017. 2
- [31] Y. Zhu, K. Sapra, F. A. Reda, K. J. Shih, S. Newsam, A. Tao, and B. Catanzaro. Improving semantic segmentation via video propagation and label relaxation. In *IEEE Conference on Computer Vision and Pattern Recognition*, 2019. 1, 2, 3